**Les Cahiers du GERAD** ISSN: 0711–2440

# Vessel service planning in seaports

ONLINE SUPPLEMENT

L. Wu, Y. Adulyasak,
J.-F. Cordeau, S. Wang

G–2020–67

November 2020



**GERAD** HEC Montréal
3000, chemin de la Côte-Sainte-Catherine
Montréal (Québec) Canada H3T 2A7

**Tél. : 514 340-6053**
Téléc. : 514 340-5665
info@gerad.ca
www.gerad.ca

# Vessel service planning in seaports

## Online supplement

**Lingxiao Wu** [a]

**Yossiri Adulyasak** [a]

**Jean-François Cordeau** [a]

**Shuaian Wang** [b]

[a] *GERAD & Département de gestion des opérations et de la logistique, HEC Montréal, Montréal (Québec), Canada, H3T 2A7*

[b] *Strome College of Business, Old Dominion University, Norfolk, Virginia 23529, USA*

lingxiaowu513@gmail.com
yossiri.adulyasak@hec.ca
jean-francois.cordeau@hec.ca
wangshuaian@gmail.com

**November 2020**
**Les Cahiers du GERAD**
**G–2020–67**

# EC1 Mathematical proofs

This section presents proofs to lemmas, propositions, theorems, and corollaries in the main text.

## EC1.1 Proof of Proposition 1

**Proof of Proposition 1.** Given any feasible solution ($\bar{\boldsymbol{\chi}}$) to the BMP, let $H = \{(i,t) | \sum_{\omega\in\Omega} \bar{\chi}_\omega \alpha_{\omega,i,t} > 0, t \in \mathcal{E}_i, i \in \mathcal{I}\}$. Given $\bar{\boldsymbol{\chi}}$, the corresponding PBSP is feasible if and only if there exists a solution $\boldsymbol{\mu}'$ such that $\sum_{\phi\in\Phi} \mu'_\phi \gamma_{\phi,i,t} = \sum_{\omega\in\Omega} \bar{\chi}_\omega \alpha_{\omega,i,t}$, $\forall (i,t) \in H$. We can show that such a $\boldsymbol{\mu}'$ exists for any $\bar{\boldsymbol{\chi}}$.

Recall that $\bigcup_{s\in\mathcal{S}} \mathcal{T}_s = \mathcal{T}$ and that all vessel routes in model M2 satisfy constraints (34). Hence, corresponding to each $(i,t) \in H$, one can always construct a feasible pilot route that visits $i$ at time $t$. In particular, the pilot route can consist of only task $i$ (which starts at time $t$) and a rest period (which starts at a feasible time) and is completed by a pilot in a suitable shift. Then, based on these pilot routes, one can easily construct a feasible solution for the PBSP.

As a result, given any $\bar{\boldsymbol{\chi}}$, the PBSP is always feasible. Furthermore, considering that the cost parameters $\bar{c}_\phi$ are finite and due to constraints (48)–(50), any feasible solution of the PBSP must be bounded. Therefore, as the dual of the PBSP, the DBSP is also feasible and bounded. □

## EC1.2 Proof of Theorem 1

**Proof of Theorem 1.** At each node of the branch-and-bound tree, the BMP and the PBSP are defined on a subset $\Omega' \subseteq \Omega$ of vessel routes and a subset $\Phi' \subseteq \Phi$ of pilot routes, due to the branching constraints. The approach solves the BMP to optimality with column-and-Benders-cut generation. Let $(\boldsymbol{\chi}^*, \eta^*)$ and $\boldsymbol{\mu}^*$ denote the optimal solution to the BMP and the associated PBSP, respectively. According to Benders (1962), we have that (i) $\boldsymbol{\chi}^*$ and $\boldsymbol{\mu}^*$ constitute an optimal solution to the LP relaxation of M2 defined on the same subsets of vessel routes and pilot routes (i.e., the LP relaxation of M2 imposed with the same branching constraints) and that (ii) the BMP and the LP relaxation of M2 have the same optimal objective function value.

Now consider our branching scheme. One can verify the solution ($\boldsymbol{\chi}^*$) generated by the C&BCG algorithm to the BMP is fractional if and only if there is at least one fractional value in $\boldsymbol{\Lambda}$ or $\boldsymbol{\Xi}$. Further, given any integer solution ($\bar{\boldsymbol{\chi}}$) for the BMP, the solution generated by column generation to the corresponding PBSP is fractional if and only if there is at least one fractional value in $\boldsymbol{\Pi}$ or $\boldsymbol{\Psi}$.

Therefore, by imposing branching constraints on the BMP and the PBSP at the associated nodes of the tree, and by solving the BMP at each node to optimality, the approach gradually reaches a solution to the BMP that has the minimum objective function value among all integer solutions (i.e., solutions where all values in the solution $\boldsymbol{\chi}^*$ are integral and all values in the solution $\boldsymbol{\mu}^*$ for the corresponding PBSP are integral as well). Correspondingly, the approach reaches an integer solution that has the minimum cost among all integer solutions for the LP relaxation of M2. Therefore, the BPBC approach delivers an optimal solution for M2. □

## EC1.3 Proof of Proposition 2

**Proof of Proposition 2.** Consider the BMP without these LBL inequalities. Given any feasible solution of the $\chi$ variables, denoted by $\bar{\boldsymbol{\chi}}$, to the BMP, let $\eta^*(\bar{\boldsymbol{\chi}})$ denote the associated optimal solution of the $\eta$ variable in the BMP. To prove that the LBL inequalities are valid for the BMP, it suffices to show that the following linear program generates a lower bound to $\eta^*(\bar{\boldsymbol{\chi}})$:

$$[\mathbf{P}_{LBL}(\bar{\boldsymbol{\chi}})] \quad \min \quad \sum_{s\in\mathcal{S}} c_s^3 n_s \tag{EC1}$$

$$\text{s.t.} \quad (69) - (72)$$

$$\sum_{s\in\mathcal{S}_t} \nu_{i,t,s} = \sum_{\omega\in\Omega} \bar{\chi}_\omega \alpha_{\omega,i,t} \qquad \forall t \in \mathcal{E}_i, i \in \mathcal{I}. \tag{EC2}$$

We have shown in Proposition 1 that the DBSP is always feasible and bounded. Given $\bar{\boldsymbol{\chi}}$, let $\boldsymbol{\delta}^*$ and $\boldsymbol{\zeta}^*$ denote an optimal solution to the DBSP. Because $(\boldsymbol{\delta}^*, \boldsymbol{\zeta}^*) \in \Gamma_\Delta$, we have $\eta^*(\bar{\boldsymbol{\chi}}) \geq \sum_{i\in\mathcal{I}}\sum_{t\in\mathcal{T}}\sum_{\omega\in\Omega}\bar{\chi}_\omega\alpha_{\omega,i,t}\delta^*_{i,t} + \sum_{\phi\in\Phi}\zeta^*_\phi$ due to constraints (56). Let $\boldsymbol{\mu}^*$ denote the optimal solution to the dual of the DBSP (i.e., the PBSP). Because of strong duality, we have $\sum_{\phi\in\Phi}\mu^*_\phi\bar{c}_\phi = \sum_{i\in\mathcal{I}}\sum_{t\in\mathcal{T}}\sum_{\omega\in\Omega}\bar{\chi}_\omega\alpha_{\omega,i,t}\delta^*_{i,t} + \sum_{\phi\in\Phi}\zeta^*_\phi$.

We construct the solution $(\boldsymbol{\nu'}, \boldsymbol{n'})$ for the variables in the $\mathrm{P}_{LBL}(\bar{\boldsymbol{\chi}})$, where

$$\nu'_{i,t,s} = \sum_{\phi\in\Phi_s}\mu^*_\phi\gamma_{\phi,i,t} \qquad \forall i\in\mathcal{I}, t\in\mathcal{T}_s, s\in\mathcal{S} \tag{EC3}$$

$$n'_s = \sum_{\phi\in\Phi_s}\mu^*_\phi \qquad \forall s\in\mathcal{S}. \tag{EC4}$$

Considering the feasibility of pilot routes and the feasibility of $\boldsymbol{\mu}^*$ for the PBSP, we have

$$\sum_{i\in\mathcal{I}}\sum_{t'} = \max\{\underline{T}_s, t-d_i-\underline{q}'_{i,t,s}+1\}^{t}\gamma_{\phi,i,t'} \leq 1, \qquad \forall t\in\mathcal{T}_s, \phi\in\Phi_s, s\in\mathcal{S} \tag{EC5}$$

$$\sum_{s\in\mathcal{S}_t}\sum_{\phi\in\Phi_s}\mu^*_\phi\gamma_{\phi,i,t} = \sum_{\omega\in\Omega}\bar{\chi}_\omega\alpha_{\omega,i,t} \qquad \forall t\in\mathcal{E}_i, i\in\mathcal{I}. \tag{EC6}$$

Because $\mu^*_\phi \geq 0$, $\forall\phi\in\Phi$, by timing each term in inequalities (EC5) with $\mu^*_\phi$, and summing them over $\phi\in\Phi_s$ we have

$$\sum_{i\in\mathcal{I}}\sum_{t'=\max\{\underline{T}_s, t-d_i-\underline{q}'_{i,t,s}+1\}}^{t}\sum_{\phi\in\Phi_s}\mu^*_\phi\gamma_{\phi,i,t'} \leq \sum_{\phi\in\Phi_s}\mu^*_\phi, \qquad \forall t\in\mathcal{T}_s, s\in\mathcal{S}. \tag{EC7}$$

Then, combining (EC3), (EC4), and (EC7) gives

$$\sum_{i\in\mathcal{I}}\sum_{t'=\max\{\underline{T}_s, t-d_i-\underline{q}'_{i,t,s}+1\}}^{t}\nu'_{i,t',s} \leq n'_s \qquad \forall t\in\mathcal{T}_s, s\in\mathcal{S}, \tag{EC8}$$

and from (EC3) and (EC6) we have

$$\sum_{s\in\mathcal{S}_t}\nu'_{i,t,s} = \sum_{\omega\in\Omega}\bar{\chi}_\omega\alpha_{\omega,i,t} \qquad \forall t\in\mathcal{E}_i, i\in\mathcal{I} \tag{EC9}$$

$$\nu'_{i,t,s} \leq 1 \qquad \forall i\in\mathcal{I}, t\in\mathcal{T}, s\in\mathcal{S} \tag{EC10}$$

$$\nu'_{i,t,s} \geq 0 \qquad \forall i\in\mathcal{I}, t\in\mathcal{T}, s\in\mathcal{S}. \tag{EC11}$$

Finally, summarizing inequalities (EC8)–(EC11), one can conclude that the constructed solution $(\boldsymbol{\nu'}, \boldsymbol{n'})$ is feasible for the $\mathrm{P}_{LBL}(\bar{\boldsymbol{\chi}})$. Besides, we have $\sum_{s\in\mathcal{S}}c^3_s n'_s = \sum_{s\in\mathcal{S}}\sum_{\phi\in\Phi_s}\bar{c}_\phi\mu^*_\phi = \sum_{\phi\in\Phi}\bar{c}_\phi\mu^*_\phi \leq \eta^*(\bar{\boldsymbol{\chi}})$. Let $(\boldsymbol{\nu^*}, \boldsymbol{n^*})$ denote an optimal solution for the $\mathrm{P}_{LBL}(\bar{\boldsymbol{\chi}})$. Because the $\mathrm{P}_{LBL}(\bar{\boldsymbol{\chi}})$ forms a minimization problem, we have $\sum_{s\in\mathcal{S}}c^3_s n^*_s \leq \sum_{s\in\mathcal{S}}c^3_s n'_s \leq \eta^*(\bar{\boldsymbol{\chi}})$.

Therefore, the $\mathrm{P}_{LBL}(\bar{\boldsymbol{\chi}})$ generates a lower bound to $\eta^*(\bar{\boldsymbol{\chi}})$, given any feasible solution of the $\chi$ variables to the original BMP. This indicates that the LBL inequalities are valid for the BMP. □

## EC1.4 Proof of Lemma 1

**Proof of Lemma 1.** We provide a proof to this lemma based on the BMP without the LBL cuts proposed in Section 4.5.1, while the extension to the BMP with these cuts is straightforward.

We start by formulating the Lagrangian dual of the BMP. Let $\bar{\boldsymbol{\pi}} = (\bar{\pi}_k | \bar{\pi}_k \in \mathbb{R}, k \in \mathcal{K})$, $\bar{\boldsymbol{\lambda}} = (\bar{\lambda}_{b,t} | \bar{\lambda}_{b,t} \leq 0, t \in \mathcal{T}, b \in \mathcal{B})$, $\bar{\boldsymbol{\theta}} = (\bar{\theta}_t | \bar{\theta}_t \leq 0, t \in \mathcal{T})$, $\bar{\boldsymbol{\vartheta}} = (\bar{\vartheta}_t | \vartheta_t \leq 0, t \in \mathcal{T})$, $\bar{\boldsymbol{\kappa}} = (\bar{\kappa}_{t,(i,j)} | \bar{\kappa}_{t,(i,j)} \leq 0, t \in \mathcal{T}, (i,j) \in \mathcal{U})$, $\bar{\boldsymbol{\varphi}} = (\bar{\varphi}_{(\boldsymbol{\delta},\boldsymbol{\zeta})} | \bar{\varphi}_{(\boldsymbol{\delta},\boldsymbol{\zeta})} \geq 0, (\boldsymbol{\delta},\boldsymbol{\zeta}) \in \Gamma_\Delta)$ and $\bar{\boldsymbol{\rho}} = (\bar{\rho}_\omega | \bar{\rho}_\omega \leq 0, \omega \in \Omega)$ be the vectors of the Lagrangian multipliers for constraints (39)–(43), (56), and (57), respectively. Besides, let $\Omega_{k,b}$ denote the set of columns corresponding to vessel $k$ being handled at berth $b$, where $k \in \mathcal{K}$, $b \in \mathcal{B}_k$. As implied by constraints (39), (57), and (58), the following inequalities are valid for the BMP:

$$\sum_{\omega \in \Omega_{k,b}} \chi_\omega \leq 1, \qquad \forall b \in \mathcal{B}_k, k \in \mathcal{K}. \tag{EC12}$$

Given $\bar{\boldsymbol{\pi}}$, $\bar{\boldsymbol{\lambda}}$, $\bar{\boldsymbol{\theta}}$, $\bar{\boldsymbol{\kappa}}$, $\bar{\boldsymbol{\varphi}}$, and $\bar{\boldsymbol{\rho}}$, the Lagrangian dual of the BMP is as follows:

$$\begin{aligned}
\mathcal{D}(\bar{\boldsymbol{\pi}}, \bar{\boldsymbol{\lambda}}, \bar{\boldsymbol{\theta}}, \bar{\boldsymbol{\kappa}}, \bar{\boldsymbol{\varphi}}, \bar{\boldsymbol{\rho}}) = \min_{\boldsymbol{\chi}, \eta} \Bigg\{ & \sum_{\omega \in \Omega} \chi_\omega c_\omega + \eta + \sum_{k \in \mathcal{K}} (1 - \sum_{\omega \in \Omega_k} \chi_\omega) \bar{\pi}_k \\
& + \sum_{t \in \mathcal{T}} \sum_{b \in \mathcal{B}} (1 - \sum_{\omega \in \Omega} \chi_\omega \sum_{t=1}^{\tau} \sum_{t'=\min\{\tau+1, \overline{T}\}}^{\overline{T}} \beta_{\omega,b,t,t'}) \bar{\lambda}_{b,t} \\
& + \sum_{t \in \mathcal{T}} (1 - \sum_{\omega \in \Omega} \chi_\omega \sum_{i \in \mathcal{I}^{in}} \sum_{t'=\max\{t-f_i+1,1\}}^{t} \alpha_{\omega,i,t'}) \bar{\theta}_t + \sum_{t \in \mathcal{T}} (1 - \sum_{\omega \in \Omega} \chi_\omega \sum_{i \in \mathcal{I}^{out}} \sum_{t'=\max\{t-f_i+1,1\}}^{t} \alpha_{\omega,i,t'}) \bar{\vartheta}_t \\
& + \sum_{t \in \mathcal{T}} \sum_{(i,j) \in \mathcal{U}} (1 - \sum_{\omega \in \Omega} \chi_\omega \sum_{t'=\max\{t-d_i+1,1\}}^{t} \alpha_{\omega,i,t'} - \sum_{\omega \in \Omega} \chi_\omega \sum_{t'=\max\{t-d_j+1,1\}}^{t} \alpha_{\omega,j,t'}) \bar{\kappa}_{t,(i,j)} \\
& - \sum_{(\boldsymbol{\delta},\boldsymbol{\zeta}) \in \Gamma_\Delta} (\eta - \sum_{i \in \mathcal{I}} \sum_{t \in \mathcal{T}} \sum_{\omega \in \Omega} \chi_\omega \alpha_{\omega,i,t} \delta_{i,t} - \sum_{\phi \in \Phi} \zeta_\phi) \bar{\varphi}_{(\boldsymbol{\delta},\boldsymbol{\zeta})} \\
& + \sum_{\omega \in \Omega} (1 - \chi_\omega) \bar{\rho}_\omega, \text{ s.t. (58), (59), (EC12)} \Bigg\}.
\end{aligned} \tag{EC13}$$

Equation (EC13) is equivalent to

$$\begin{aligned}
\mathcal{D}(\bar{\boldsymbol{\pi}}, \bar{\boldsymbol{\lambda}}, \bar{\boldsymbol{\theta}}, \bar{\boldsymbol{\kappa}}, \bar{\boldsymbol{\varphi}}, \bar{\boldsymbol{\rho}}) = & \sum_{k \in \mathcal{K}} \bar{\pi}_k + \sum_{t \in \mathcal{T}} \sum_{b \in \mathcal{B}} \bar{\lambda}_{b,t} + \sum_{t \in \mathcal{T}} \bar{\theta}_t + \sum_{t \in \mathcal{T}} \bar{\vartheta}_t + \sum_{t \in \mathcal{T}} \sum_{(i,j) \in \mathcal{U}} \bar{\kappa}_{t,(i,j)} + \sum_{(\boldsymbol{\delta},\boldsymbol{\zeta}) \in \Gamma_\Delta} \sum_{\phi \in \Phi} \zeta_\phi \bar{\varphi}_{(\boldsymbol{\delta},\boldsymbol{\zeta})} \\
& + \sum_{\omega \in \Omega} \bar{\rho}_\omega + \min_{\boldsymbol{\chi}, \eta} \Bigg\{ \sum_{\omega \in \Omega} \chi_\omega c_\omega + (1 - \sum_{(\boldsymbol{\delta},\boldsymbol{\zeta}) \in \Gamma_\Delta} \bar{\varphi}_{(\boldsymbol{\delta},\boldsymbol{\zeta})}) \eta - \sum_{k \in \mathcal{K}} \sum_{\omega \in \Omega_k} \chi_\omega \bar{\pi}_k \\
& - \sum_{t \in \mathcal{T}} \sum_{b \in \mathcal{B}} \sum_{\omega \in \Omega} \chi_\omega \sum_{t=1}^{\tau} \sum_{t'=\min\{\tau+1, \overline{T}\}}^{\overline{T}} \beta_{\omega,b,t,t'} \bar{\lambda}_{b,t} \\
& - \sum_{t \in \mathcal{T}} \sum_{\omega \in \Omega} \chi_\omega \sum_{i \in \mathcal{I}^{in}} \sum_{t'=\max\{t-f_i+1,1\}}^{t} \alpha_{\omega,i,t'} \bar{\theta}_t - \sum_{t \in \mathcal{T}} \sum_{\omega \in \Omega} \chi_\omega \sum_{i \in \mathcal{I}^{out}} \sum_{t'=\max\{t-f_i+1,1\}}^{t} \alpha_{\omega,i,t'} \bar{\vartheta}_t \\
& - \sum_{t \in \mathcal{T}} \sum_{(i,j) \in \mathcal{U}} \sum_{\omega \in \Omega} \chi_\omega \sum_{t'=\max\{t-d_i+1,1\}}^{t} \alpha_{\omega,i,t'} \bar{\kappa}_{t,(i,j)} - \sum_{\omega \in \Omega} \chi_\omega \sum_{t'=\max\{t-d_j+1,1\}}^{t} \alpha_{\omega,j,t'} \bar{\kappa}_{t,(i,j)} \\
& + \sum_{(\boldsymbol{\delta},\boldsymbol{\zeta}) \in \Gamma_\Delta} \sum_{i \in \mathcal{I}} \sum_{t \in \mathcal{T}} \sum_{\omega \in \Omega} \chi_\omega \alpha_{\omega,i,t} \delta_{i,t} \bar{\varphi}_{(\boldsymbol{\delta},\boldsymbol{\zeta})} - \sum_{\omega \in \Omega} \chi_\omega \bar{\rho}_\omega, \text{ s.t. (58), (59), (EC12)} \Bigg\}.
\end{aligned} \tag{EC14}$$

Let $Z^*$ be the optimal objective function value for the BMP. We have

$$Z^* \geq \max_{\bar{\boldsymbol{\pi}}, \bar{\boldsymbol{\lambda}}, \bar{\boldsymbol{\theta}}, \bar{\boldsymbol{\kappa}}, \bar{\boldsymbol{\varphi}}, \bar{\boldsymbol{\rho}}} \mathcal{D}(\bar{\boldsymbol{\pi}}, \bar{\boldsymbol{\lambda}}, \bar{\boldsymbol{\theta}}, \bar{\boldsymbol{\kappa}}, \bar{\boldsymbol{\varphi}}, \bar{\boldsymbol{\rho}}). \tag{EC15}$$

Since the BMP is solved by column and Benders cut generation, where columns and Benders cuts are added dynamically, we let $\tilde{\Omega} \subseteq \Omega$ and $\tilde{\Gamma}_\Delta \subseteq \Gamma_\Delta$ denote the current sets of columns and Benders cuts generated for solving the BMP, respectively. After solving the BMP with columns from $\tilde{\Omega}$ and Benders cuts from $\tilde{\Gamma}_\Delta$, one obtains the optimal solutions to the dual variables associated with constraints (39)–(43), (56), and (57) which are denoted by $\boldsymbol{\pi}^* = (\pi_k^* | k \in \mathcal{K})$, $\boldsymbol{\lambda}^* = (\lambda_{b,t}^* | t \in \mathcal{T}, b \in \mathcal{B})$, $\boldsymbol{\theta}^* = (\theta_t^* | t \in \mathcal{T})$, $\boldsymbol{\vartheta}^* = (\vartheta_t^* | t \in \mathcal{T})$, $\boldsymbol{\kappa}^* = (\kappa_{t,(i,j)}^* | t \in \mathcal{T}, (i,j) \in \mathcal{U})$, $\boldsymbol{\varphi}^* = (\varphi_{(\boldsymbol{\delta},\boldsymbol{\zeta})}^* | (\boldsymbol{\delta},\boldsymbol{\zeta}) \in \tilde{\Gamma}_\Delta)$, and $\boldsymbol{\rho}^* = (\rho_\omega^* | \omega \in \tilde{\Omega})$, respectively. We further define vectors $\boldsymbol{\varphi}^+$ and $\boldsymbol{\rho}^+$ such that $\boldsymbol{\varphi}^+ = (\varphi_{(\boldsymbol{\delta},\boldsymbol{\zeta})}^+ | \varphi_{(\boldsymbol{\delta},\boldsymbol{\zeta})}^+ = \varphi_{(\boldsymbol{\delta},\boldsymbol{\zeta})}^*, (\boldsymbol{\delta},\boldsymbol{\zeta}) \in \tilde{\Gamma}_\Delta, \varphi_{(\boldsymbol{\delta},\boldsymbol{\zeta})}^+ = 0, (\boldsymbol{\delta},\boldsymbol{\zeta}) \in \Gamma_\Delta \setminus \tilde{\Gamma}_\Delta)$ and $\boldsymbol{\rho}^+ = (\rho_\omega^+ | \rho_\omega^+ = \rho_\omega^*, \omega \in \tilde{\Omega}, \rho_\omega^+ = 0, \omega \in \Omega \setminus \tilde{\Omega})$.

By definition, the BMP is constructed to be feasible and bounded. As a result, the dual of BMP is also feasible and bounded. By the feasibility of the dual of the BMP, one can easily verify that $(\boldsymbol{\pi}^*, \boldsymbol{\lambda}^*, \boldsymbol{\theta}^*, \boldsymbol{\vartheta}^*, \boldsymbol{\kappa}^+, \boldsymbol{\varphi}^+)$ forms a feasible solution for $\mathcal{D}(\bar{\boldsymbol{\pi}}, \bar{\boldsymbol{\lambda}}, \bar{\boldsymbol{\theta}}, \bar{\boldsymbol{\kappa}}, \bar{\boldsymbol{\varphi}}, \bar{\boldsymbol{\rho}})$. It follows that

$$Z^* \geq \mathcal{D}(\boldsymbol{\pi}^*, \boldsymbol{\lambda}^*, \boldsymbol{\theta}^*, \boldsymbol{\vartheta}^*, \boldsymbol{\kappa}^*, \boldsymbol{\varphi}^+, \boldsymbol{\rho}^+), \tag{EC16}$$

where

$$\begin{aligned}
\mathcal{D}(\boldsymbol{\pi}^*, \boldsymbol{\lambda}^*, \boldsymbol{\theta}^*, \boldsymbol{\vartheta}^*, \boldsymbol{\kappa}^*, \boldsymbol{\varphi}^+, \boldsymbol{\rho}^+) = {} & \sum_{k\in\mathcal{K}} \pi_k^* + \sum_{t\in\mathcal{T}}\sum_{b\in\mathcal{B}} \lambda_{b,t}^* + \sum_{t\in\mathcal{T}} \theta_t^* + \sum_{t\in\mathcal{T}} \vartheta_t^* + \sum_{t\in\mathcal{T}}\sum_{(i,j)\in\mathcal{U}} \kappa_{t,(i,j)}^* \\
& + \sum_{(\boldsymbol{\delta},\boldsymbol{\zeta})\in\tilde{\Gamma}_\Delta}\sum_{\phi\in\Phi} \zeta_\phi \varphi_{(\boldsymbol{\delta},\boldsymbol{\zeta})}^* + \sum_{\omega\in\tilde{\Omega}} \rho_\omega^* + \min_{\boldsymbol{\chi},\eta} \Bigg\{ \sum_{\omega\in\Omega} \chi_\omega c_\omega + (1 - \sum_{(\boldsymbol{\delta},\boldsymbol{\zeta})\in\tilde{\Gamma}_\Delta} \varphi_{(\boldsymbol{\delta},\boldsymbol{\zeta})}^*)\eta - \sum_{k\in\mathcal{K}}\sum_{\omega\in\Omega_k} \chi_\omega \pi_k^* \\
& - \sum_{t\in\mathcal{T}}\sum_{b\in\mathcal{B}}\sum_{\omega\in\Omega} \chi_\omega \sum_{t=1}^{\tau} \sum_{t'=\min\{\tau+1,\overline{T}\}}^{\overline{T}} \beta_{\omega,b,t,t'} \lambda_{b,t}^* \\
& - \sum_{t\in\mathcal{T}}\sum_{\omega\in\Omega} \chi_\omega \sum_{i\in\mathcal{I}^{in}} \sum_{t'=\max\{t-f_i+1,1\}}^{t} \alpha_{\omega,i,t'} \theta_t^* - \sum_{t\in\mathcal{T}}\sum_{\omega\in\Omega} \chi_\omega \sum_{i\in\mathcal{I}^{out}} \sum_{t'=\max\{t-f_i+1,1\}}^{t} \alpha_{\omega,i,t'} \vartheta_t^* \\
& - \sum_{t\in\mathcal{T}}\sum_{(i,j)\in\mathcal{U}}\sum_{\omega\in\Omega} \chi_\omega \sum_{t'=\max\{t-d_i+1,1\}}^{t} \alpha_{\omega,i,t'} \kappa_{t,(i,j)}^* - \sum_{\omega\in\Omega} \chi_\omega \sum_{t'=\max\{t-d_j+1,1\}}^{t} \alpha_{\omega,j,t'} \kappa_{t,(i,j)}^* \\
& + \sum_{(\boldsymbol{\delta},\boldsymbol{\zeta})\in\tilde{\Gamma}_\Delta}\sum_{i\in\mathcal{I}}\sum_{t\in\mathcal{T}}\sum_{\omega\in\Omega} \chi_\omega \alpha_{\omega,i,t} \delta_{i,t} \varphi_{(\boldsymbol{\delta},\boldsymbol{\zeta})}^* - \sum_{\omega\in\tilde{\Omega}} \chi_\omega \rho_\omega^*, \text{ s.t. } (58), (59), (\text{EC12}) \Bigg\}.
\end{aligned} \tag{EC17}$$

Due to the feasibility of the dual of the BMP, we have $\sum_{(\boldsymbol{\delta},\boldsymbol{\zeta})\in\tilde{\Gamma}_\Delta} \varphi_{(\boldsymbol{\delta},\boldsymbol{\zeta})}^* \leq 1$ and $\rho_\omega^* \leq 0$, $\forall \omega \in \tilde{\Omega}$. Further, considering that $\eta \geq 0$ and $\chi_\omega \geq 0$, $\forall \omega \in \tilde{\Omega}$, we have $(1 - \sum_{(\boldsymbol{\delta},\boldsymbol{\zeta})\in\tilde{\Gamma}_\Delta} \varphi_{(\boldsymbol{\delta},\boldsymbol{\zeta})}^*)\eta \geq 0$ and $\sum_{\omega\in\tilde{\Omega}} \chi_\omega \rho_\omega^* \leq 0$. Recall that in this lemma, the optimal objective function value of the BMP is denoted by $\Upsilon$. By strong duality, we have $\Upsilon = \sum_{k\in\mathcal{K}} \pi_k^* + \sum_{t\in\mathcal{T}}\sum_{b\in\mathcal{B}} \lambda_{b,t}^* + \sum_{t\in\mathcal{T}} \theta_t^* + \sum_{t\in\mathcal{T}} \vartheta_t^* + \sum_{t\in\mathcal{T}}\sum_{(i,j)\in\mathcal{U}} \kappa_{t,(i,j)}^* + \sum_{(\boldsymbol{\delta},\boldsymbol{\zeta})\in\tilde{\Gamma}_\Delta}\sum_{\phi\in\Phi} \zeta_\phi \varphi_{(\boldsymbol{\delta},\boldsymbol{\zeta})}^* + \sum_{\omega\in\tilde{\Omega}} \rho_\omega^*$. Therefore, we have the following inequality:

$$\begin{aligned}
\mathcal{D}(\boldsymbol{\pi}^*, \boldsymbol{\lambda}^*, \boldsymbol{\theta}^*, \boldsymbol{\vartheta}^*, \boldsymbol{\kappa}^*, \boldsymbol{\varphi}^+, \boldsymbol{\rho}^+) \geq \mathcal{D}' = \Upsilon + \min_{\boldsymbol{\chi}} \Bigg\{ & \sum_{\omega\in\Omega} \chi_\omega (c_\omega - \pi_k^* - \sum_{t\in\mathcal{T}}\sum_{t=1}^{\tau} \sum_{t'=\min\{\tau+1,\overline{T}\}}^{\overline{T}} \beta_{\omega,b,t,t'} \lambda_{b,t}^* \\
& - \sum_{t\in\mathcal{T}}\sum_{i\in\mathcal{I}^{in}\cap\mathcal{I}_k} \sum_{t'=\max\{t-f_i+1,1\}}^{t} \alpha_{\omega,i,t'} \theta_t^* - \sum_{t\in\mathcal{T}}\sum_{i\in\mathcal{I}^{out}\cap\mathcal{I}_k} \sum_{t'=\max\{t-f_i+1,1\}}^{t} \alpha_{\omega,i,t'} \vartheta_t^* \\
& - \sum_{t\in\mathcal{T}}\sum_{i\in\mathcal{I}_k}\sum_{j\in\mathcal{I}}\sum_{(i,j)\in\mathcal{U}} \sum_{t'=\max\{t-d_i+1,1\}}^{t} \alpha_{\omega,i,t'} \kappa_{t,(i,j)}^* \\
& + \sum_{(\boldsymbol{\delta},\boldsymbol{\zeta})\in\tilde{\Gamma}_\Delta}\sum_{i\in\mathcal{I}_k}\sum_{t\in\mathcal{T}}\sum_{\omega\in\Omega} \chi_\omega \alpha_{\omega,i,t} \delta_{i,t} \varphi_{(\boldsymbol{\delta},\boldsymbol{\zeta})}^*), \text{ s.t. } (58), (\text{EC12}) \Bigg\}.
\end{aligned} \tag{EC18}$$

Considering that $\Omega = \bigcup_{k\in\mathcal{K}}\bigcup_{b\in\mathcal{B}_k}\Omega_{k,b}$ and by decomposing the minimization problem in (EC18) for each combination of $b$ and $k$, where $k \in \mathcal{K}$, $b \in \mathcal{B}_k$, $\mathcal{D}'$ can be equivalently calculated by:

$$\begin{aligned}\mathcal{D}' = \Upsilon + \sum_{k\in\mathcal{K}}\sum_{b\in\mathcal{B}_k}\min_{\chi_\omega:\omega\in\Omega_{k,b}}\sum_{\omega\in\Omega_{k,b}}\Bigg\{&\chi_\omega(c_\omega - \pi_k^* - \sum_{t\in\mathcal{T}}\sum_{t=1}^{\tau}\sum_{t'=\min\{\tau+1,\overline{T}\}}^{\overline{T}}\beta_{\omega,b,t,t'}\lambda_{b,t}^*\\ &-\sum_{t\in\mathcal{T}}\sum_{i\in\mathcal{I}^{in}\cap\mathcal{I}_k}\sum_{t'=\max\{t-f_i+1,1\}}^{t}\alpha_{\omega,i,t'}\theta_t^* - \sum_{t\in\mathcal{T}}\sum_{i\in\mathcal{I}^{out}\cap\mathcal{I}_k}\sum_{t'=\max\{t-f_i+1,1\}}^{t}\alpha_{\omega,i,t'}\vartheta_t^*\\ &-\sum_{t\in\mathcal{T}}\sum_{i\in\mathcal{I}_k}\sum_{j\in\mathcal{I}}\sum_{(i,j)\in\mathcal{U}}\sum_{t'=\max\{t-d_i+1,1\}}^{t}\alpha_{\omega,i,t'}\kappa_{t,(i,j)}^* + \sum_{(\boldsymbol{\delta},\boldsymbol{\zeta})\in\bar{\Gamma}_\Delta}\sum_{i\in\mathcal{I}_k}\sum_{t\in\mathcal{T}}\sum_{\omega\in\Omega}\chi_\omega\alpha_{\omega,i,t}\delta_{i,t}\varphi^*_{(\boldsymbol{\delta},\boldsymbol{\zeta})}),\\ &\text{s.t.}\sum_{\omega\in\Omega_{k,b}}\chi_\omega \le 1,\ \ 0\le\chi_\omega\le 1,\ \ \forall\omega\in\Omega_{k,b}\Bigg\}. \end{aligned} \tag{EC19}$$

Let $r_{k,b}$ be the optimal objective function value of the pricing problem $\text{MPP}_{k,b}$, where $k \in \mathcal{K}$, $b \in \mathcal{B}_k$. It can be readily seen that

$$\mathcal{D}' = \Upsilon + \sum_{k\in\mathcal{K}}\sum_{b\in\mathcal{B}_k:r_{k,b}<0} r_{k,b}. \tag{EC20}$$

Summarizing (EC16), (EC18), and (EC20), we have $Z^* \ge \Upsilon + \sum_{k\in\mathcal{K}}\sum_{b\in\mathcal{B}_k:r_{k,b}<0} r_{k,b}$, which completes the proof. □

## EC1.5 Proof of Proposition 3

**Proof of Proposition 3.** Let $LB = \Upsilon + \sum_{k\in\mathcal{K}}\sum_{b\in\mathcal{B}_k:r_{k,b}<0} r_{k,b}$. From Lemma 1, we have that $LB$ is a lower bound for the BMP at the current node. Given a pair of $b \in \mathcal{B}$ and $k \in \mathcal{K}$ that satisfies the conditions in this proposition, the lower bound (denoted by $LB'$) of the BMP with the constraint $\sum_{\omega\in\Omega_{k,b}}\chi_\omega = 1$ at the current node can be calculated by

$$\begin{aligned}LB' = LB + \min_{\omega\in\Omega_{k,b}}\Bigg\{&c_\omega - \pi_k^* - \sum_{t\in\mathcal{T}}\sum_{t=1}^{\tau}\sum_{t'=\min\{\tau+1,\overline{T}\}}^{\overline{T}}\beta_{\omega,b,t,t'}\lambda_{b,t}^*\\ &-\sum_{t\in\mathcal{T}}\sum_{i\in\mathcal{I}^{in}\cap\mathcal{I}_k}\sum_{t'=\max\{t-f_i+1,1\}}^{t}\alpha_{\omega,i,t'}\theta_t^* - \sum_{t\in\mathcal{T}}\sum_{i\in\mathcal{I}^{out}\cap\mathcal{I}_k}\sum_{t'=\max\{t-f_i+1,1\}}^{t}\alpha_{\omega,i,t'}\vartheta_t^*\\ &-\sum_{t\in\mathcal{T}}\sum_{i\in\mathcal{I}_k}\sum_{j\in\mathcal{I}}\sum_{(i,j)\in\mathcal{U}}\sum_{t'=\max\{t-d_i+1,1\}}^{t}\alpha_{\omega,i,t'}\kappa_{t,(i,j)}^* + \sum_{(\boldsymbol{\delta},\boldsymbol{\zeta})\in\bar{\Gamma}_\Delta}\sum_{i\in\mathcal{I}_k}\sum_{t\in\mathcal{T}}\sum_{\omega\in\Omega}\chi_\omega\alpha_{\omega,i,t}\delta_{i,t}\varphi^*_{(\boldsymbol{\delta},\boldsymbol{\zeta})}\Bigg\}, \end{aligned}$$

which equals $LB + r_{k,b}$.

Therefore, $LB + r_{k,b}$ is a lower bound for the BMP with the constraint $\sum_{\omega\in\Omega_{k,b}}\chi_\omega = 1$ at the current node. It follows easily that $LB + r_{k,b}$ is also a lower bound for the BMP with the constraint $\sum_{\omega\in\Omega_{k,b}}\chi_\omega = 1$ at any node descended from the current node. □

## EC1.6 Proof of Proposition 4

**Proof of Proposition 4.** Given any solution to the BMP, denoted by $\bar{\boldsymbol{\chi}}$, the PBSP at node $\iota'$ is a relaxation of that at node $\iota$. Accordingly, given $\bar{\boldsymbol{\chi}}$, the DBSP at node $\iota$ is a relaxation of that at node $\iota'$. Hence, any point in the polyhedron defined by (52)–(54) of the DBSP at node $\iota'$ is also in the polyhedron defined by (52)–(54) of the DBSP at node $\iota$. As a result, according to Benders (1962), the Benders cuts that are valid for the BMP at node $\iota'$ are also valid for the BMP at node $\iota$. □

### EC1.7 Proof of Corollary 1

**Proof of Corollary 1.** For the root node (denoted by $\iota_0$), we have $\Theta_{\iota_0} = \varnothing$. Hence, we have that for any node $\iota \neq \iota_0$, $\Theta_{\iota_0} \subseteq \Theta_\iota$. Therefore, according to Proposition 4, Benders cuts that are valid for the BMP at the root node are also valid for the BMP at any other node in the branch-and-bound tree. □

## EC2 The label correcting algorithm for solving the SPP$_s$

This section describes the label correcting algorithm for solving the pricing problems in the Dantzig-Wolfe decomposition of the PBSP. Consider the pricing problem corresponding to shift $s$ (SPP$_s$). The label correcting algorithm aims to identify the path, denoted by $\mathscr{P}_s^*$ in the space-time network $G_s$ that has the minimum cost (denoted by $\tilde{c}_s^*$).

In the algorithm, $H_s$ is partitioned into two subsets: $H_s^1 = \{(i,t)|t + d_i \leq \overline{L}_s, (i,t) \in H_s\}$ and $H_s^2 = \{(i,t)|t \geq \underline{L}_s + g_s, (i,t) \in H_s\}$ (a node $(i,t)$ can appear in both subsets). Observe that $H_s^1$ contains all tasks that can start before the rest period in shift $s$, whereas $H_s^2$ contains all tasks that can start after the rest period. Each $(i,t) \in H_s^1$ is associated with a label $l_{(i,t)}^1 = (\tilde{c}_{(i,t)}^1, V_{(i,t)}^1)$, where $V_{(i,t)}^1$ is the list of nodes that are visited before or at time $t$ in the label and $\tilde{c}_{(i,t)}^1$ is the associated cost. Similarly, each $(i,t) \in H_s^2$ is associated with a label $l_{(i,t)}^2 = (\tilde{c}_{(i,t)}^2, V_{(i,t)}^2)$, where $V_{(i,t)}^2$ is the list of nodes that are visited after or at time $t$ in the label and $\tilde{c}_{(i,t)}^2$ is the associated cost.

The algorithm generates $\mathscr{P}_s^*$ in three steps. The first step, which is called forward label correcting, generates the $l_{(i,t)}^1$ with the minimum cost $\tilde{c}_{(i,t)}^1$ for each $(i,t) \in H_s^1$. The second step, which is called backward label correcting, generates the $l_{(i,t)}^2$ with the minimum cost $\tilde{c}_{(i,t)}^2$ for each $(i,t) \in H_s^2$. Finally, $\mathscr{P}_s^*$ is constructed in the last step, which is called label joining and route construction. The details of these steps are presented in Sections EC2.1, EC2.2 and EC2.3, respectively. We prove the correctness of the label correcting algorithm for solving the SPP$_s$ and discuss its time complexity in Proposition 1 which is presented in Section EC.2.3.

### EC2.1 Forward label correcting

In forward label correcting, for each node $(i,t) \in H_s^1$, we find the minimum-cost (partial) path that ends at this node. To this end, we first sequence all nodes in set $H_s^1$ in non-decreasing order according to their start times $(t)$, where ties are broken arbitrarily. Let $(i_h, t_h)$, $h = 1, ..., |H_s^1|$ denote the $h$-th node in the sequence. The details of this procedure are presented in Algorithm EC.1.

**Algorithm EC.1** Forward label correcting.

Initialization: $l_{(i,t)}^1 = (-\delta_{i,t}, [(i,t)])$, $\forall (i,t) \in H_s^1$.
Sequence $(i,t) \in H_s^1$ in non-decreasing order of $t$.
**for** $h = 1, ..., |H_s^1| - 1$ **do**
  **for** $h' = h+1, ..., |H_s^1|$ **do**
    **if** $i_h \neq i_{h'}$ & $t_h + d_{i_h} + q_{i_h,i_{h'}} \leq t_{h'}$ **then**
      **if** $\tilde{c}_{(i_h,t_h)}^1 - \delta_{i_{h'},t_{h'}} \leq \tilde{c}_{(i_{h'},t_{h'})}^1$ **then**
        $\tilde{c}_{(i_{h'},t_{h'})}^1 = \tilde{c}_{(i_h,t_h)}^1 - \delta_{i_{h'},t_{h'}}$.
        $V_{(i_{h'},t_{h'})}^1 = V_{(i_h,t_h)}^1 \leftarrow (i_{h'},t_{h'})$. ▷ Operator "$\leftarrow$" represents adding an element to the rear of a list.
      **end if**
    **end if**
  **end for**
**end for**
Return $l_{(i,t)}^1$, $\forall (i,t) \in H_s^1$.

## EC2.2 Backward label correcting

In backward label correcting, for each node $(i,t) \in H_s^2$, we find the minimum-cost (partial) path that starts from this node. To this end, we first sequence all nodes in set $H_s^2$ in non-decreasing order according to their start times ($t$), where ties are broken arbitrarily. Let $(i_h, t_h)$, $h = 1, ..., |H_s^2|$ denote the $h$-th node in the sequence. The details of this procedure are presented in Algorithm EC.2.

**Algorithm EC.2** Backward label correcting.

Initialization: $l^2_{(i,t)} = (-\delta_{i,t}, [(i,t)])$, $\forall (i,t) \in H_s^2$.
Sequence $(i,t) \in H_s^2$ in non-decreasing order of $t$.
**for** $h = |H_s^2|, ..., 2$ **do**
  **for** $h' = h-1, ..., 1$ **do**
    **if** $i_h \neq i_{h'}$ & $t_{h'} + d_{i_{h'}} + q_{i_{h'}, i_h} \leq t_h$ **then**
      **if** $\tilde{c}^2_{(i_h,t_h)} - \delta_{i_{h'},t_{h'}} \leq \tilde{c}^2_{(i_{h'},t_{h'})}$ **then**
        $\tilde{c}^2_{(i_{h'},t_{h'})} = \tilde{c}^2_{(i_h,t_h)} - \delta_{i_{h'},t_{h'}}$.
        $V^2_{(i_{h'},t_{h'})} = [(i_{h'},t_{h'})] \leftarrow V^2_{(i_h,t_h)}$.
      **end if**
    **end if**
  **end for**
**end for**
Return $l^2_{(i,t)}$, $\forall (i,t) \in H_s^2$.

## EC2.3 Label joining and route construction

In the last step, we identify the pilot route with the minimum cost ($\mathscr{P}_s^*$) by constructing and searching among three sets of pilot routes, including (i) the set of routes that terminate at the rest period, (ii) the set of routes that start from the rest period, and (iii) the set of routes where the rest period serves as an intermediate node. Algorithm EC.3 shows the pseudo-code of this procedure, where we let $j$ denote the rest period.

**Proposition 1** *The label correcting algorithm solves the SPP$_s$ in $\mathcal{O}(|H_s|^2)$ time.*

**Proof.** We first prove the correctness of the algorithm. In the first step of the algorithm, we aim to find, for each node $(i,t) \in H_s^1$, the minimum-cost (partial) path that ends at this node. All nodes in $H_s^1$ have been sequenced in non-decreasing order of $t$, and it is only possible for a path to travel from node $(i,t)$ to another node $(i',t')$, if $t' \geq t$. Therefore, for the first node in the sequence, i.e., $(i_1, t_1)$, the minimum cost and the minimum-cost path have been contained in the label $l^1_{(i,t)}$ after initialization. Next, consider the two-layer for-loop in Algorithm EC.1. Because routes can only travel through the nodes chronologically, when $h = 1$ in the first layer, the algorithm finds the optimal label $l^1_{(i_2,t_2)}$ for node $(i_2, t_2)$ in the second layer. By induction, we can prove that the algorithm finds the best label for node $(i_{\bar{h}+1}, t_{\bar{h}+1})$ when $h = \bar{h}$ in the for-loop. This indicates that Algorithm EC.1 can identify the minimum-cost (partial) path that ends at each node $(i,t) \in H_s^1$ after executing the for-loop.

Following a similar logic, one can prove that Algorithm EC.2 generates the minimum-cost (partial) path that starts from each node $(i,t) \in H_s^2$.

Because $H_s^1$ (resp. $H_s^2$) contains all nodes that can be visited before (resp. after) the rest period starts in a pilot route, by comparing the labels corresponding to all nodes in $H_s^1$ (resp. $H_s^2$), Algorithm EC.3 finds the pilot route with the minimum cost that terminates at (resp. starts from) the rest period. Finally, by concatenating all compatible pairs of labels corresponding to nodes from $H_s^1$ and $H_s^2$, Algorithm EC.3 finds the pilot route with the minimum cost where the rest period is an intermediate node.

As for the time complexity of the algorithm, in Algorithms EC.1 and EC.2, it takes $\mathcal{O}(|H_s| \log |H_s|)$ time and $\mathcal{O}(|H_s|^2)$ time, respectively, to sequence the nodes in $H_s^1$ and $H_s^2$ and correct their labels.

In Algorithms EC.3, the optimal pilot routes from the three sets are generated in $\mathcal{O}(|H_s|)$, $\mathcal{O}(|H_s|)$, and $\mathcal{O}(|H_s|^2)$ time, respectively. It can be readily seen that the overall time complexity for the label correcting algorithm is $\mathcal{O}(|H_s|^2)$. □

**Algorithm EC.3** Label joining and pilot route construction.

Initialization: $\tilde{c}_s^* = M$. ▷ $M$ is a sufficiently large constant.
**for** $(i,t) \in H_s^1$ **do**
  **if** $\tilde{c}_s^* > \tilde{c}_{(i,t)}^1 + c_s^3$ **then**
    $\tilde{c}_s^* = \tilde{c}_{(i,t)}^1 + c_s^3$.
    $\mathscr{P}_s^* = V_{i,t}^1 \leftarrow (j, \overline{L}_s)$. ▷ $(j, \overline{L}_s)$ represents starting the rest period at time step $\overline{L}_s$.
  **end if**
**end for**
**for** $(i,t) \in H_s^2$ **do**
  **if** $\tilde{c}_s^* > \tilde{c}_{(i,t)}^2 + c_s^3$ **then**
    $\tilde{c}_s^* = \tilde{c}_{(i,t)}^2 + c_s^3$.
    $\mathscr{P}_s^* = [(j, \underline{L}_s)] \leftarrow V_{i,t}^2$. ▷ $(j, \underline{L}_s)$ represents starting the rest period at time step $\underline{L}_s$.
  **end if**
**end for**
**for** $(i,t) \in H_s^1$ **do**
  **for** $(i',t') \in H_s^2$ **do**
    **if** $i \neq i'$ & $t + d_i + q_{i,i'} \leq t'$ **then**
      $t_j = \min\{t + d_i, \underline{L}_s\}$. ▷ Find the earliest feasible start time for the rest period.
      **if** $t_j + g_s \leq t'$ **then** ▷ Recall that $g_s$ denote the minimum duration for a rest period in shift $s$.
        **if** $\tilde{c}_s^* > \tilde{c}_{(i,t)}^1 + \tilde{c}_{(i',t')}^2 + c_s^3$ **then**
          $\tilde{c}_s^* = \tilde{c}_{(i,t)}^1 + \tilde{c}_{(i',t')}^2 + c_s^3$.
          $\mathscr{P}_s^* = V_{(i,t)}^1 \leftarrow (j, t_j) \leftarrow V_{(i',t')}^2$. ▷ $(j, t_j)$ represents starting the rest period at time step $t_j$.
        **end if**
      **end if**
    **end if**
  **end for**
**end for**
Return $\mathscr{P}_s^*$ and $\tilde{c}_s^*$.

## EC3 The pricing problems for the BMP with the LBL cuts

In this section, we explain the pricing problems for the BMP with the LBL cuts.

Let $\boldsymbol{\varpi} = (\varpi_{s,t} | t \in \mathcal{T}_s, s \in \mathcal{S})$ denote vector of dual variables associated with constraints (72). New vessel routes are generated by solving a pricing problem (denoted by $\text{MPP}'_{k,b}$) for each $k \in \mathcal{K}$ and $b \in \mathcal{B}_k$. The $\text{MPP}'_{k,b}$ can be defined as a problem that identifies the arc with the minimum cost in a three-dimensional task-time-shift network $G'_{k,b} = (N'_{k,b}, A'_{k,b})$, where $N'_{k,b}$ and $A'_{k,b}$ denote the sets of nodes and arcs in the network, respectively. Here, $N'_{k,b} = \{(i,t,s) | s \in \mathcal{S}_t, t \in \mathcal{E}_i, i \in \mathcal{I}_k\}$ and $A'_{k,b} = \{[(i,t,s),(i',t',s')] | t' - t \geq d_i + h_{k,b}, (i,t,s), (i',t',s') \in N'_{k,b}, i \in \mathcal{I}^{in}, i \in \mathcal{I}^{out}\}$. The cost of sending a unit flow through arc $[(i,t,s),(i',t',s')]$, denoted by $\hat{c}'_{[(i,t,s),(i',t',s')]}$, is calculated by

$$\hat{c}'_{[(i,t,s),(i',t',s')]} = \hat{c}_{[(i,t),(i',t')]} + \sum_{\tau=t}^{\min\{t+d_i+\underline{q}'_{i,t,s}-1, \overline{T}_s\}} \varpi_{s,\tau} + \sum_{\tau=t'}^{\min\{t'+d_{i'}+\underline{q}'_{i',t',s'}-1, \overline{T}_{s'}\}} \varpi_{s',\tau}, \quad \text{(EC21)}$$

where $\hat{c}_{[(i,t),(i',t')]}$ is calculated by (60).

## EC4 The heuristic for generating integer solutions

In this section, we explain the heuristic that tries to construct a feasible integer solution for M2 from a fractional solution. Let $\boldsymbol{\chi}^0$ and $\boldsymbol{\mu}^0$ denote the optimal (fractional) solution to the BMP and PBSP at

a node in the branch-and-bound tree, respectively. The heuristic consists of three stages. In the first stage, we try to construct a feasible integer solution (denoted by $\boldsymbol{\chi}^1$) for the BMP (without the Benders cuts (56)). If such a solution can be constructed, then in the second step, we solve the associated PBSP using column generation. Let $\boldsymbol{\mu}^1$ denote the solution to the PBSP. If $\boldsymbol{\mu}^1$ is fractional, we construct an integer solution (denoted by $\boldsymbol{\mu}^2$) based on $\boldsymbol{\mu}^1$ in the last step. Note that if $\boldsymbol{\chi}^0$ is integral then we skip the first stage and let $\boldsymbol{\chi}^1 = \boldsymbol{\chi}^0$ and if $\boldsymbol{\mu}^1$ is integral then we skip the third stage and let $\boldsymbol{\mu}^2 = \boldsymbol{\mu}^1$. Corresponding to each feasible integer solution for M2 generated by the heuristic, we obtain a valid upper bound which equals $\sum_{\omega\in\Omega} \chi^1_\omega \bar{c}_\omega + \sum_{\phi\in\Phi} \mu^2_\phi \bar{c}_\phi$. Details of the first and the third stages in the heuristic are explained as follows.

## EC4.1 Constructing vessel routes

Given a fractional solution ($\boldsymbol{\chi}^0$) to the BMP, we apply a greedy algorithm to construct a feasible integer solution ($\boldsymbol{\chi}^1$) for the BMP without the Benders cuts (56). The algorithm leverages information from the current fractional solution. Let $\Omega^+ = \{\omega | \chi^0_\omega > 0, \omega \in \Omega\}$ and let $\mathbb{S}_{\Omega^+}$ denote a sequence which lists elements in $\Omega^+$ in non-decreasing order of $\chi^0_\omega$. We let $\omega_\varrho$, $\varrho = 1, 2, ..., |\Omega^+|$ denote the $\varrho$-th element in $\mathbb{S}_{\Omega^+}$. The procedure for constructing $\boldsymbol{\chi}^1$ is presented in Algorithm EC.4, and we make use of the following additional notation in the pseudo-code:

- $k(\omega)$: The vessel $k \in \mathcal{K}$ associated with vessel route $\omega$.
- $b(\omega)$: The berth $b \in \mathcal{B}$ used in vessel route $\omega$.
- $i^{in}(\omega)$: The task $i \in \mathcal{I}^{in}$ covered in vessel route $\omega$.
- $i^{out}(\omega)$: The task $i \in \mathcal{I}^{out}$ covered in vessel route $\omega$.
- $t_1(\omega)$: The time step $t \in \mathcal{T}$ when the vessel in $\omega$ starts sailing into its berth.
- $t_2(\omega)$: The time step $t \in \mathcal{T}$ when the vessel in $\omega$ reaches its berth.
- $t_3(\omega)$: The time step $t \in \mathcal{T}$ when the vessel in $\omega$ leaves its berth.
- $\bar{\mathcal{K}}$: Set of vessels that have associated vessel routes in $\Omega^1$.
- $\bar{\mathcal{T}}^{in}$: Set of time steps at which vessels cannot start sailing into berths.
- $\bar{\mathcal{T}}^{out}$: Set of time steps at which vessels cannot start sailing out of berths.
- $\tilde{\mathcal{T}}_i$: Set of time steps at which task $i \in \mathcal{I}$ cannot start.
- $\hat{\mathcal{T}}_b$: Set of time steps at which berth $b \in \mathcal{B}$ is occupied by vessels.

One can easily verify that if $|\bar{\mathcal{K}}| = |\mathcal{K}|$, then by letting $\chi^1_\omega = 1$, $\forall \omega \in \Omega^1$, and $\chi^1_\omega = 0$, $\forall \omega \in \Omega \setminus \Omega^1$, $\boldsymbol{\chi}^1$ becomes a feasible integer solution for the BMP (without Benders cuts). Meanwhile, observe that it is also possible that Algorithm EC.4 fails to generate a feasible integer solution. In this case, the primal heuristic fails to find a valid upper bound for M2.

## EC4.2 Constructing pilot routes

Given a feasible integer solution ($\boldsymbol{\chi}^1$) to the BMP, we solve the associated PBSP using column generation. Suppose the delivered solution to the PBSP, denoted by $\boldsymbol{\mu}^1$, is fractional. In this case, to construct a feasible integer solution for the PBSP (denoted by $\boldsymbol{\mu}^2$), we use an algorithm that is similar to the algorithm for generating vessel routes in the previous section. The algorithm can generate a feasible integer solution for the PBSP given any feasible integer solution for the BMP ($\boldsymbol{\chi}^1$). The details are explained as follows.

Constructing $\boldsymbol{\mu}^2$ is equivalent to generating a set $\Phi^2 \subseteq \Phi$ such that $\mu^2_\phi = 1$, $\forall \phi \in \Phi^2$ and $\mu^2_\phi = 0$, $\forall \phi \in \Phi \setminus \Phi^2$. Algorithm EC.6 presents the details of the procedure. In the algorithm, we let $\Phi^+ = \{\phi | \mu^1_\phi > 0, \phi \in \Phi\}$, and let $\mathbb{S}_{\Phi^+}$ denote a sequence that lists the elements in $\Phi^+$ in non-decreasing order of $\mu^1_\phi$. Besides, let $\phi_\varrho$, $\varrho = 1, 2, ..., |\Phi^+|$ denote the $\varrho$-th element in $\mathbb{S}_{\Phi^+}$. The following notation is also used in the pseudo-code: $s(\phi)$ which denotes the shift associated with pilot route $\phi$, $\mathcal{I}(\phi)$ which denotes the set of tasks covered in pilot route $\phi$, and $\bar{\mathcal{I}}$ which denotes the set of tasks that have been covered by pilot routes in $\Phi^2$.

**Algorithm EC.4** Vessel route construction.

Initialization: $\Omega^1 = \varnothing$; $\bar{\mathcal{K}} = \bar{\mathcal{T}}^{in} = \bar{\mathcal{T}}^{out} = \varnothing$; $\hat{\mathcal{T}}_b = \varnothing$, $b \in \mathcal{B}$; $\tilde{\mathcal{T}}_i = \varnothing$, $i \in \mathcal{I}$.
**for** $\varrho = 1, 2, ..., |\Omega^+|$ **do**
  **if** $k(\omega_\varrho) \notin \bar{\mathcal{K}}$ & $t_1(\omega_\varrho) \notin \bar{\mathcal{T}}^{in}$ & $t_3(\omega_\varrho) \notin \bar{\mathcal{T}}^{out}$ & $t_1(\omega_\varrho) \notin \tilde{\mathcal{T}}_{i^{in}(\omega_\varrho)}$ & $t_3(\omega_\varrho) \notin \tilde{\mathcal{T}}_{i^{out}(\omega_\varrho)}$ & $\mathbb{Z}_{[t_2(\omega_\varrho), t_3(\omega_\varrho)-1]} \cap \hat{\mathcal{T}}_{b(\omega_\varrho)} = \varnothing$ **then**
    $\bar{\mathcal{K}} = \bar{\mathcal{K}} \cup \{k(\omega_\varrho)\}$. ▷ Update the set of vessels that have been included in the solution.
    $\Omega^1 = \Omega^1 \cup \{\omega_\varrho\}$. ▷ Update the set of vessel routes that have been included in the solution.
    Call sub-procedure $\mathbf{P}(\omega)$ in Algorithm EC.5. ▷ Update the constraints.
  **end if**
  **if** $|\bar{\mathcal{K}}| = |\mathcal{K}|$ **then**
    Break.
  **end if**
**end for**
**for** $k \in \mathcal{K} \setminus \bar{\mathcal{K}}$ **do** ▷ Construct routes for vessels not included in the current solution; $k$ are enumerated chronologically according to their earliest ready times for entering the channel.
  **for** $t_1 \in \mathcal{E}_{i^{in}}$ **do** ▷ $i^{in} \in \mathcal{I}_k \cap \mathcal{I}^{in}$. $t_1$ are enumerated chronologically.
    **for** $t_3 \in \mathcal{E}_{i^{out}}$ **do** ▷ $i^{out} \in \mathcal{I}_k \cap \mathcal{I}^{out}$. $t_3$ are enumerated chronologically.
      **if** $t_1 \notin \bar{\mathcal{T}}^{in}$ & $t_3 \notin \bar{\mathcal{T}}^{out}$ & $t_1 \notin \tilde{\mathcal{T}}_{i^{in}}$ & $t_3 \notin \tilde{\mathcal{T}}_{i^{out}}$ **then**
        **for** $b \in \mathcal{B}_k$ **do** ▷ $b$ are enumerated in non-increasing order of $c^2_{k,b}$.
          $t_2 = t_1 + d_{i^{in}}$.
          **if** $t_2 \geq a_b$ & $t_2 + h_{k,b} \leq t_3$ & $\mathbb{Z}_{[t_2, t_3-1]} \cap \hat{\mathcal{T}}_b = \varnothing$ **then**
            Construct a vessel route $\omega$ such that $k(\omega) = k$, $b(\omega) = b$, $t_1(\omega) = t_1$, $t_2(\omega) = t_2$, $t_3(\omega) = t_3$, and $\bar{c}_\omega = c^1_{i^{in}, t_1} + c^1_{i^{out}, t_3} + c^2_{k,b}$.
            $\bar{\mathcal{K}} = \bar{\mathcal{K}} \cup \{k\}$.
            $\Omega^1 = \Omega^1 \cup \{\omega\}$.
            Call sub-procedure $\mathbf{P}(\omega)$ in Algorithm EC.5.
            Break and **go to** Line 12.
          **end if**
        **end for**
      **end if**
    **end for**
  **end for**
**end for**
Return $\Omega^1$.

**Algorithm EC.5** Constraint update $[\mathbf{P}(\omega)]$.

$\bar{\mathcal{T}}^{in} = \bar{\mathcal{T}}^{in} \cup \mathbb{Z}_{[t_1(\omega), t_1(\omega)+f_{i^{in}(\omega)}-1]}$. ▷ Update time steps at which vessels cannot start sailing into the berths.
$\hat{\mathcal{T}}_{b_\omega} = \hat{\mathcal{T}}_{b_\omega} \cup \mathbb{Z}_{[t_2(\omega), t_3(\omega)-1]}$. ▷ Update time steps at which the berth is occupied.
$\bar{\mathcal{T}}^{out} = \bar{\mathcal{T}}^{out} \cup \mathbb{Z}_{[t_3(\omega), t_3(\omega)+f_{i^{out}(\omega)}-1]}$. ▷ Update time steps at which vessels cannot start sailing out of the berths.
**for** $j \in I$ **do** ▷ Update time steps at which a task cannot start due to the non-simultaneity constraints (43).
  **if** $(i^{in}(\omega), j) \in \mathcal{U}$ **then**
    $\tilde{\mathcal{T}}_j = \tilde{\mathcal{T}}_j \cup \mathbb{Z}_{[t_1(\omega), t_1(\omega)+d_{i^{in}(\omega)}-1]}$.
  **end if**
  **if** $(i^{out}(\omega), j) \in \mathcal{U}$ **then**
    $\tilde{\mathcal{T}}_j = \tilde{\mathcal{T}}_j \cup \mathbb{Z}_{[t_3(\omega), t_3(\omega)+d_{i^{out}(\omega)}-1]}$.
  **end if**
**end for**
Return $\bar{\mathcal{T}}^{in}$, $\bar{\mathcal{T}}^{out}$, $\hat{\mathcal{T}}_b$, $b \in \mathcal{B}$, $\tilde{\mathcal{T}}_i$, $i \in \mathcal{I}$.

# EC5 Data of the Hong Kong container port and parameter settings in the instances

## EC5.1 Data of the port

We generated the instances based on real operational data from the Hong Kong Container Port. The physical layout of the port is depicted in Figure EC1(a). There are 24 berths in the Kwai Tsing Container Terminals. More than 85% of all vessel arrivals in this port travel through the East Lamma Channel, which is a bidirectional channel with two traffic lanes: one for incoming vessels and the other for outgoing vessels. Due to its sufficient water depth, vessels of all sizes can sail in the channel at any

**Algorithm EC.6** Pilot route construction.

Initialization: $\Phi^2 = \varnothing$; $\bar{\mathcal{I}} = \varnothing$.
**for** $\varrho = 1, 2, ..., |\Phi^+|$ **do**
  $\mathcal{I}' = \varnothing$.
  **for** $i \in \mathcal{I}(\phi_\varrho)$ **do**
    **if** $i \notin \bar{\mathcal{I}}$ **then**
      $\mathcal{I}' = \mathcal{I}' \cup \{i\}$.
    **end if**
  **end for**
  **if** $\mathcal{I}' \neq \varnothing$ **then**
    $\bar{\mathcal{I}} = \bar{\mathcal{I}} \cup \mathcal{I}'$.
    Construct a pilot route $\phi' \in \Phi_{s(\phi)}$ that covers all tasks in $\mathcal{I}'$; ▷ Route $\phi'$ can be generated by letting all tasks in $\mathcal{I}'$ and the rest period start at the same times as they do in route $\phi_\varrho$; The cost of the route equals $\bar{c}_{\phi'} = c^3_{s(\phi)}$.
    $\Phi^2 = \Phi^2 \cup \{\phi'\}$.
  **end if**
  **if** $|\bar{\mathcal{I}}| = |\mathcal{I}|$ **then**
    Break.
  **end if**
**end for**
Return $\Phi^2$.

time of the day (i.e., there is no tidal window for vessels in the channel). There is a pilot boarding station at the entrance of the channel where pilots can board or deboard vessels. The port also has an anchorage located near the East Lamma Channel, where arriving vessels can wait before sailing into the channel.

To better explain the movements of vessels in the port, in Figure EC1(b), we illustrate the locations of vessels in the port at a given time and the trajectory of a vessel that was handled in the port. This figure was adapted from a screenshot of a software application that monitors real-time vessel positions and movements in the Hong Kong Container Port.

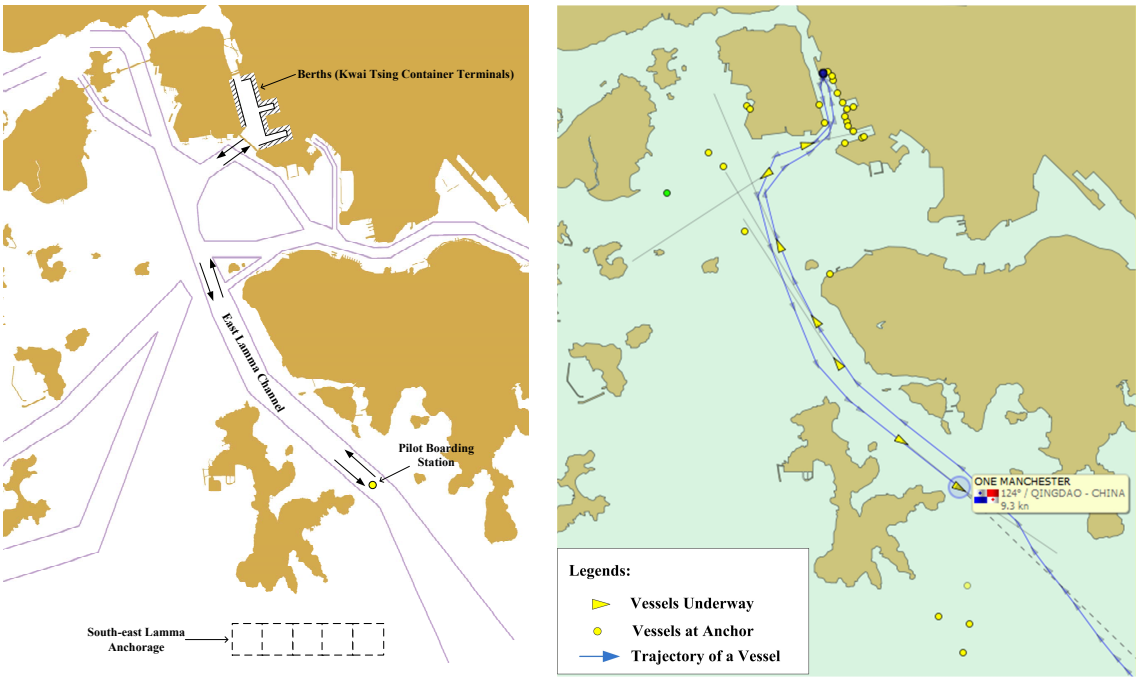


(a) Port Layout. (b) Vessel Traffic.

**Figure EC1: Layout of the Hong Kong container port and an illustration of vessel traffic in the port.**

In 2017, 10,633 vessel arrivals were handled in the port (The Marine Department of Hong Kong 2018), which translates to approximately 1.21 vessel arrivals per berth per day on average. To derive the vessel service data, we collected messages sent by the onboard Automatic Identification System (AIS) of the vessels handled in the Hong Kong Container Port in 2017. The AIS is to vessels what GPS is to cars. The reader is referred to Yang et al. (2019) for more information on the AIS and AIS messages. By leveraging the AIS data, we obtained 7,062 complete vessel arrival records. Each record depicts the movements of a vessel (accurate to one minute) during its entire port stay. For each of the arrivals, we identified (i) the capacity of the associated vessel, (ii) the handling time at the berths, and (iii) the transit time between the pilot boarding station and the berths.

Table EC1 reports the distribution of the vessel capacities associated with the 7,062 vessel arrivals. We classify vessels into five groups according to their capacities (in twenty-foot equivalent units, or TEU): feeder, intermediate (S), intermediate (L), large, and jumbo. We present the distribution of handling times (in hours) of different vessels in Figure EC2. Among the 7,062 vessel arrivals, 6,425 and 5,655 arrivals entered and departed the port through the East Lamma Channel, respectively. The average traveling time between the berths and the pilot boarding station in the channel was 64 minutes, and nearly 80% of transit times lay within the range of [54,72] minutes.

**Table EC1: Distribution of vessel capacities.**

| Type | Size (TEU) | Number | Ratio (%) |
|---|---|---|---|
| Feeder | [500, 3000] | 3815 | 54% |
| Intermediate (S) | [3001, 6000] | 1710 | 24% |
| Intermediate (L) | [6001, 9000] | 988 | 14% |
| Large | [9001, 12000] | 229 | 3% |
| Jumbo | [12001, 18500] | 320 | 5% |

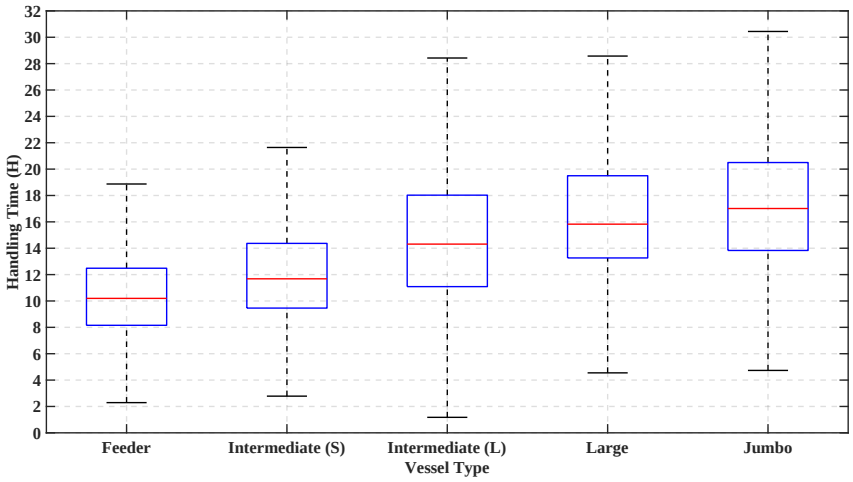


**Figure EC2: Distribution of vessel handling times.**

Pilotage is compulsory in Hong Kong; all vessels over 3,000 gross tons must have a pilot on board when navigating in the port (the smallest container vessel in our record is over 8,900 gross tons). There are approximately 100 pilots licensed to serve vessels in Hong Kong (The Marine Department of Hong Kong 2020a). To board vessels, pilots travel in the port using pilot boats. Pilot boats are significantly smaller than container vessels; the typical length of a pilot boat is between 12 and 14 meters, whereas the smallest feeder container vessel in our record is 138 meters long. While the speed of container vessels in the channel is normally between 10–15 knots, pilot boats can travel at much higher speeds (up to a maximum of 30 knots) in port waters. Accordingly, pilot boats can overtake container vessels when sailing in the channel. A pilot boat can travel between any two berths in the port within 5 minutes and between berths and the pilot boarding station within 20 minutes.

## EC5.2 Parameter settings in the instances

Based on the operational data of the Hong Kong Container Port, we generate parameters in our testing instances as follows.

First, corresponding to the five vessel types listed in Table EC1, we classify vessels in the instances into five grades: Grades I, II, III, IV, and V. A higher grade indicates larger capacities. Among all vessels calling at the seaport in an instance, the probabilities of the vessels being of Grades I, II, III, IV, and V are set to 54%, 24%, 14%, 3%, and 5%, respectively. Vessels arrive at the seaport dynamically and uniformly throughout the planning horizon. In the instances, a vessel can be handled at any berth in the seaport, and the cargo handling times for vessel $k$ at all berths are set to be identical and equal to $\hat{h}_k$. Here, $\hat{h}_k$ is randomly generated using the uniform distributions $U(8,12)$, $U(10,14)$, $U(11,18)$, $U(13,20)$, and $U(14,21)$ (in hours) for vessels of Grades I, II, III, IV, and V, respectively.

Second, requirements regarding channel traffic management in the instances are set as follows. The time for a vessel to travel between the anchorage and berths (including sailing in the channel and berthing into or unberthing from a berth), denoted by $\hat{d}$, is set to 70 minutes. There should be a minimum headway between any two vessels that sail in the same direction in the channel. Meanwhile, large-sized vessels cannot sail in opposite directions in the channel simultaneously. However, the exact minimum headway and non-simultaneity requirements in the Hong Kong Container Port are not available to us. In the instances, we set the minimum headway to be 10 minutes, which is in accordance with the setting used by Jia et al. (2019). We also stipulate that vessels of Grade IV or V cannot sail in opposite directions in the channel simultaneously.

Third, the time windows of the pilotage tasks are set in such a way as to fulfill the following two requirements: (i) any incoming vessel should start sailing into the berths no more than eight hours after arrival, and (ii) the total turnaround time of vessel $k$ should not exceed the sum of the sailing time between the anchorage and the berths and the handling time ($2\hat{d} + \hat{h}_k$), plus a total buffer time of 16 hours.

Fourth, given that seaports operate around the clock, we simulate the initial condition in the seaport as follows. We set the probability of a berth being occupied by a vessel to $0.5R$ ($R$ denotes the vessel arrival rate [vessel arrivals per berth per day]). For an occupied berth, the probabilities of it being occupied by a Grade I, II, III, IV, and V vessel are set to 54%, 24%, 14%, 3%, and 5%, respectively. If a berth is occupied, its available time (counting from the beginning of the planning horizon) is generated from $U(1,10)$ (in hours); otherwise, we set the available time to zero. Meanwhile, to impose the minimum headway requirement, no vessels in the instances can leave their berths within the first 10 minutes after an initially occupied berth becomes available. Moreover, to impose the non-simultaneity requirements between large vessels, if a berth is occupied by a Grade IV or V vessel, no Grade IV or V vessels in the instances can start sailing into the berths within the first 70 minutes after the berth becomes available. To impose these requirements, the time windows of the pilotage tasks for the vessels are adjusted accordingly.

Fifth, in each instance, each pilot working in a shift is awarded a rest period that should last at least an hour and cannot start within the first 30% or the last 30% period in the shift. A pilot can maneuver multiple vessels in a shift, and a minimum setup time is required to reposition a pilot between two tasks. If the repositioning does not necessitate travel through the channel, we set the minimum setup time to 10 minutes; otherwise, we set the minimum setup time to 30 minutes.

Sixth, because we consider a discrete-time problem, the time points (for defining various time windows) and time durations (of tasks, rest periods, and vessel handling) generated in continuous time are translated into parameters depicted by discrete time steps. Such translation is conducted by applying the appropriate ceiling or flooring operators on the continuous-time parameters to ensure the feasibility of the obtained discrete-time solutions for the original continuous-time instances.

Finally, we set the cost components as follows. First, tasks that start later than their earliest possible start times are punished. The unit-time delay cost for tasks corresponding to vessels of Grades I, II, III, IV, and V sailing into berths are set to 2, 3, 4, 5, and 6, respectively. The unit-time delay cost for tasks corresponding to vessels of Grades I, II, III, IV, and V leaving berths are set to 4, 6, 8, 10, and 12, respectively. Meanwhile, the cost for handling vessel $k$ at berth $b$ is set to $c^2_{k,b} = \lceil 5 o_b \hat{h}_k \rceil$, where $o_b$ is generated from $U(1, 1.5)$. Finally, the cost paid by the port authority for assigning a pilot to work in a shift is set to 48 (i.e., 1 per unit time).

## References

Jia S, Li CL, Xu Z (2019) Managing navigation channel traffic and anchorage area utilization of a container port. Transportation Science 53(3):728–745.

The Marine Department of Hong Kong (2018) Port of Hong Kong Statistical Tables 2017. Technical report, https://www.mardep.gov.hk/en/publication/pdf/portstat_ast_2017.pdf, Accessed Sepetember 1, 2020.

The Marine Department of Hong Kong (2020) Pilotage in Hong Kong. https://www.mardep.gov.hk/en/pub_services/ocean/pilot.html, Accessed November 18, 2020.

Yang D, Wu L, Wang S, Jia H, Li KX (2019) How big data enriches maritime research–a critical review of automatic identification system (AIS) data applications. Transport Reviews 39(6):755–773.